Available online at www.sciencedirect.com

ScienceDirect

Procedia Structural Integrity 18 (2019) 651–656

Structural Integrity Procedia

www.elsevier.com/locate/procedia

25th International Conference on Fracture and Structural Integrity

Assessment of the fatigue performance of heat-treated addictive manufactured TiAl6V4 specimens

L.P. Borrego[a,b]*, J. de Jesus[a], J.A.M. Ferreira[a], J.D.M. Costa[a], C. Capela[a,c]

[a] *CEMMPRE, Department of Mechanical Enginnering, University of Coimbra, 3004-516 Coimbra, Portugal*
[b] *Coimbra Polytechnic - ISEC, Rua Pedro Nunes, 3030-199 Coimbra, Portugal*
[c] *ESTG,Mechanical Engineering Department, Polytechnic Institute of Leiria, Portugal*

Abstract

Titanium Ti6Al4V alloy has excellent mechanical properties and corrosion resistance combined with low specific weight, and is commonly used in biomedical applications, automotive and aerospace components, involving fatigue loadings. Current work studies the fatigue behavior under strain amplitude control of titanium TiAl6V4 specimens, intending to characterize fatigue strength from low to high life range after different heat treatments. Fatigue tests were carried out at room temperature, using round dog bone specimens produced by selective laser melting (SLM), where laser powder deposition occurred in layers perpendicular to the loading direction. Two batches of specimens were tested: one subjected to a stress relieve treatment and a second one treated by the hot isostatic pressing process (HIP). The material was characterized in terms of the tensile mechanical properties, cycle curve, Basquin and Coffin equations. Additional analysis of the hardness and scanning electron microscopy was carried out to complement the discussion of the results. The obtained dada showed that the stress relieved specimens exhibits significantly cyclic softening, increasing with applied strain, while HIP specimens show a practically stable cyclic behavior in relation to the monotonic curve. Material response for both treatments is well fitted by Basquin and Coffin-Manson formulations. The transition life was 187 reversals and 326 reversals, for stress relieved and HIP specimens, respectively. Fatigue life for a given strain is governed by the strain value, independently of the post manufacturing heat treatment.

Peer-review under responsibility of the Gruppo Italiano Frattura (IGF) ExCo.

Keywords: Additive manufacturing; Fatigue strength; Low cycle fatigue; TiAl6V4 alloy.

* Corresponding author. Tel.: +351239790200; fax: +351239790331.
E-mail address: borrego@isec.pt

2452-3216
Peer-review under responsibility of the Gruppo Italiano Frattura (IGF) ExCo.
10.1016/j.prostr.2019.08.212

1. Introduction

Additive manufacturing (AM) is a technique increasingly used for producing complex metal components, particularly the Ti6Al4V alloy widely used in biomedical and aerospace components and other high-performance engineering applications, as reported by Petrovic et al. (2011) and Mur et al. (2010). Taking in account the excellent mechanical properties and with low specific weight, the use of this process in the automotive and aerospace industries, lead to weight reduction and decreasing use of energy, Guo and Leu (2013) and Frazier (2014).

Fatigue performance of additive manufactured TiAl6V4 alloy, is significantly influenced by porosities, different heat treatments and surface conditions. Edwards and Ramulu (2014) and Greitmeier et al. (2015) reported the effect of the heat treatment on the fatigue limit. Leuders et al. (2013) and Rafi et al. (2013) studied also the improvement of the fatigue performance on AM TiAl6V4 alloy promoted by the reduction of defects due to optimized process parameters or by hot isostatic pressing (HIP). Leuders et al. (2013) report the effect of the heat treatment temperature on the mechanical properties of TiAl6V4 alloy produced by selective laser melting (SLM), showing an increasing in break elongation and a decreasing of the ultimate strength with the temperature of the heat treatment. The same authors stated that the effect of the heat treatment on mechanical properties in driven by three causes:

- the reduction of internal stress without changing of microstructure (observed for short heat-treatment on a low temperature level);
- changing of microstructure (for higher temperature level or a longer time for heat treatment);
- changing of microstructure combined with the reduction of pores (which occurs for hot isostatic pressing).

The benefit effect of the hot isostatic pressing was also observed on retardation of the fatigue crack propagation, particularly nearly threshold, by Greitmeier et al. (2017).

Nomenclature

AM	Additive manufacturing
HIP	Hot isostatic pressing
SLM	Selective laser melting
b	Fatigue strength exponent
c	Fatigue ductility exponent
k’	Cyclic hardening coefficient
n’	Cyclic hardening exponent
N_f	Number of cycles to failure
$\sigma_{f'}$	Fatigue strength coefficient
$\epsilon_{f'}$	Fatigue ductility coefficient

2. Material and testing

Experimental tests were performed using dog bone round specimens, with final geometry and dimensions shown in Fig. 1, synthesized by Lasercusing®, with layers growing towards the direction of loading application. The samples were processed in a 3DSystems DMP ProX320 high-performance metal additive manufacturing machine, incorporating a 500w fiber laser, using an energy density of 57J/mm^3 and 30 μm layer thickness. Metal powder was the Titanium Ti6Al4V Grade 23 alloy, with a chemical composition indicated in Table 1, according with the manufacturer.

Two batches of specimens were produced applying different heat treatments, after a mechanical polishing of the surfaces, with the purpose of reducing the residual stresses and the internal porosity. The stress relieve treatment consisted of slow and controlled heating up to 670 °C, followed by maintenance at 670 °C±15 ºC for 5 hours in argon medium at atmosphere pressure and a finally by cooling to room temperature in air. The HIP treatment, consisted of slow and controlled heating up to 920 °C, followed by maintenance for 2 hours at this temperature, in argon medium at a pressure of 100 MPa, and finally subjected to a controlled cooling in until achieving less than 150 ºC.

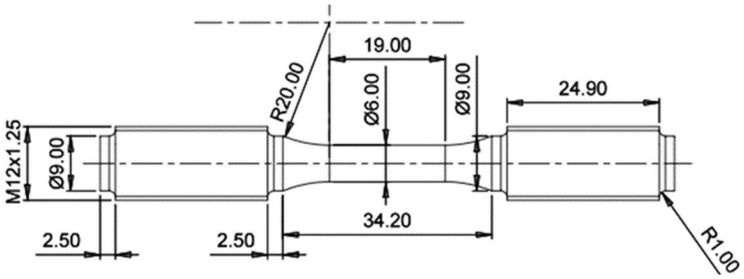

Fig. 1. Geometry of the specimens (dimensions in mm).

Two types of fatigue tests were performed, in air at room temperature and with sinusoidal waveforms, using a Dartec 100 KN servo-hydraulic mechanical testing machine. Low cycle fatigue tests were carried out, according to the recommendations of ASTM E606 standard, under fully reversed strain-controlled conditions (R_ε = -1), and a constant strain rate ($d\varepsilon/dt$) of 8×10^{-3} s^{-1}. Long life tests were performed with R_ε = -1 and at a frequency of 5 Hz.

The specimens were cut in planes containing the longitudinal axle, prepared according to the standard metallographic practice and subjected to a chemical attack by Kroll`s reagent. After preparation, the samples were observed using a Leica DM4000 M LED optical microscope. For both heat treatments, the microstructure reveals a fine acicular morphology mainly the primary α phase or α' (martensite) heterogeneously dispersed. The β phase appears distributed in α, especially in the contours of the grains. HIP treatments morphology, shown in Fig. 2 presents only a significant coarse lamellar microstructure. This morphology is quite similar to that observed by Greitmeier et al. (2017) for similar material and manufacturing conditions.

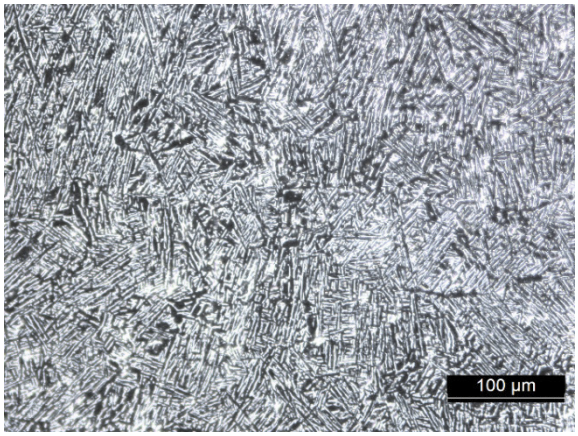

Fig. 2. Microstructure of the HIP samples.

Table 2 presents the ultimate tensile strength average values, obtained by tensile tests, for both heat treatments. During low cycle fatigue tests, the strain control and monitoring was done using a 12.5 mm-long gauge extensometer (model Instron 2620-601, Instron, Norwood, MA, USA). The gauge was directly clamped to the specimens via two separated knife-edges, and connected to a digital data acquisition system.

Table 1. Chemical composition of the Titanium Ti6Al4V alloy [wt.%].

Al	V	O	N	C	H	Fe	Y	Ti
5.50 - 6.50	3.50 - 4.50	< 0.15	< 0.04	< 0.08	< 0.012	< 0.25	< 0.005	Bal.

3. Results and discussion

The stresses and strains were continuously monitored during all tests. Fig. 3 presents the variations of the peak stresses against the life ratio N/N_f, (where N is the current number of cycles and N_f is the number of cycles to failure), at various strain amplitude levels, for HIP specimens. For high strain amplitude levels, it was observed that the peak stresses decreases in an initial stage (increasing with the strain level), and afterwards there is a very slow reduction until the final failure. However, for the low strain levels no material softening was observed.

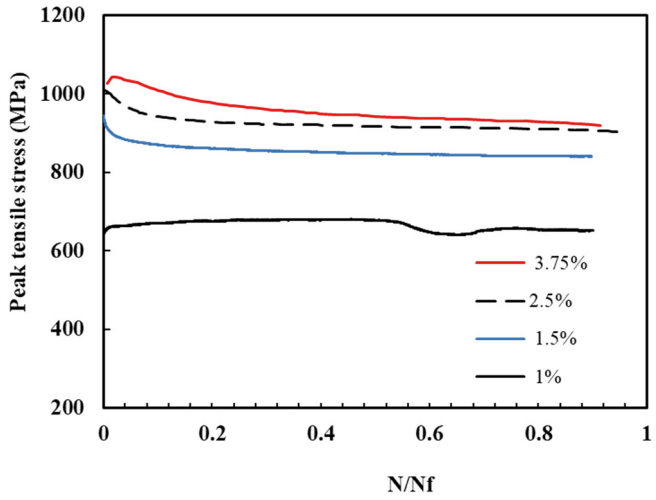

Fig. 3. Peak stress against normalized fatigue life for HIP specimens.

The cyclic stress-strain response was analyzed for all low cycle fatigue tests. Fig. 4 shows the evolution of the cyclic stress-strain curves in early transient regime for one HIP specimen tested at a strain range of 2.5%. A significant cyclic softening of the material was observed during the first 20 cycles, followed by a stabilization of the hysteresis curves.

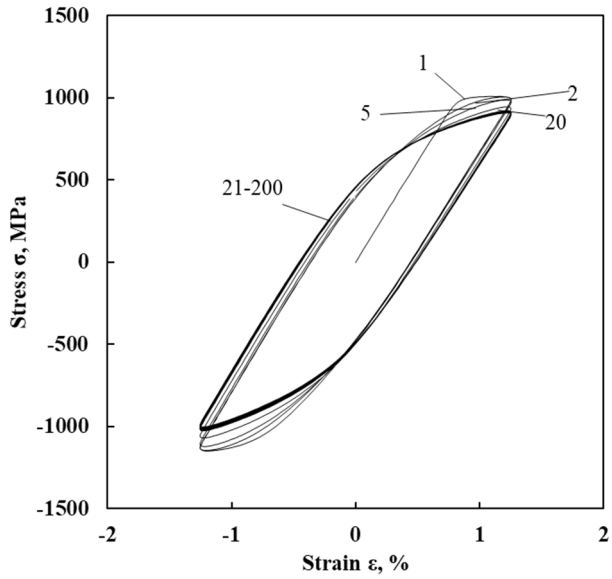

Fig. 4. Cyclic stress-strain curves for one HIP specimen tested at 2% of strain amplitude.

Assuming the fact that the saturated regime is achieved in the early stage of the tests, cyclic curve was obtained via the data collected from the hysteresis loops at half-life. Figures 5a) and 5b) display the monotonic stress-strain curves and superimposes the cycle curves, for stress relieved and HIP specimens, respectively. For stress relieved specimens, it was observed that the cyclic curve is significantly lower the than monotonic one in the plastic region, indicating cyclic softening of the material for that strain levels. However, for HIP specimens the two curves are quite close, not showing significant cyclic behavior change in relation to the monotonic one. The cyclic stress-strain curve was fitted by the Ramberg-Osgood equation. Table 2 presents the values obtained for k' and n', which are the cyclic hardening coefficient and exponent, respectively.

Fatigue results were analyzed in terms of elastic, plastic, and total strain amplitudes against the number of reversals to failure. Experimental results were fitted by the well-known Basquin and Coffin-Manson formulations, where: σ_f' is the fatigue strength coefficient, b is the fatigue strength exponent, ε_f' is the fatigue ductility coefficient, c is the fatigue ductility coefficient and N_f is the number of cycles to failure. The values obtained for these parameters are indicated in Table 2 for both treatments. The transition life obtained for this alloy was quite low, 187 reversals and 326 reversals, for stress relieved and HIP specimens, respectively, which can be attributed to the combination of high strength and relatively low ductility.

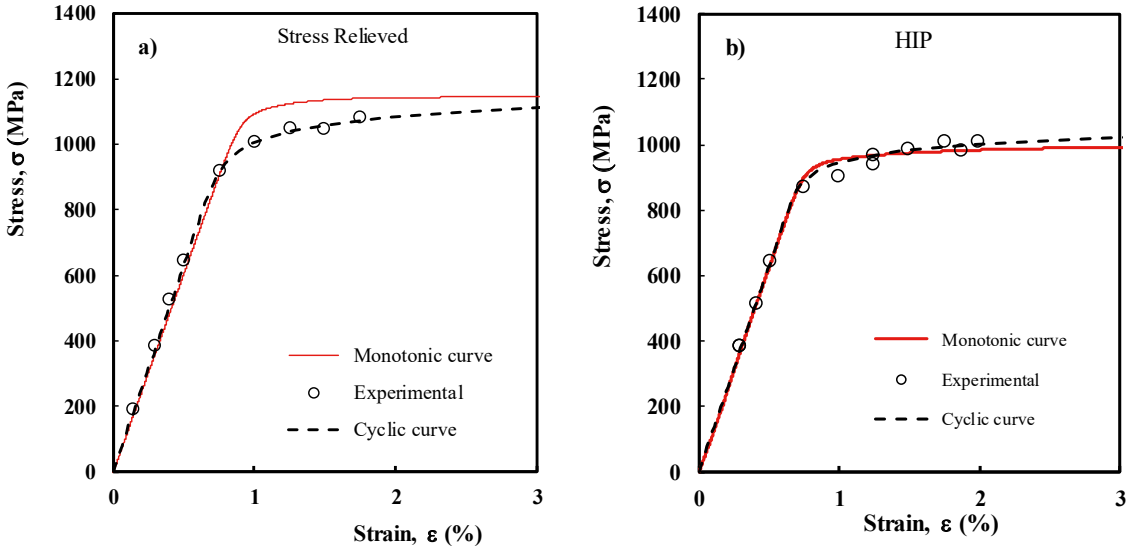

Fig. 5. Comparison of cyclic and monotonic stress-strain curves: a) Stress relieved; b) HIP treatment.

Table 2. Mechanical properties of Ti6Al4V alloy after treatments.

Treatment	Ultimate strength (MPa)	Hardness (HV_1)	k' (MPa)	n'
Stress relieved	1144	405	1314	0.0432
HIP	995	350	1176	0.0364
Treatment	σ_f' (MPa)	b	ε_f' (%)	c
Stress relieved	3055.6	-0.163	89.380	-0.853
HIP	2115.1	-0.129	67.164	-0.764

In order to compare the fatigue performance of both treatments, the results of the total strain amplitudes against the number of cycles to failure, were superimposes as shown in Fig. 6. In spite, significant differences observed in the cycle behavior for both treatments, fatigue life for a given strain is governed mainly by the strain value, independently of the post manufacturing heat treatment.

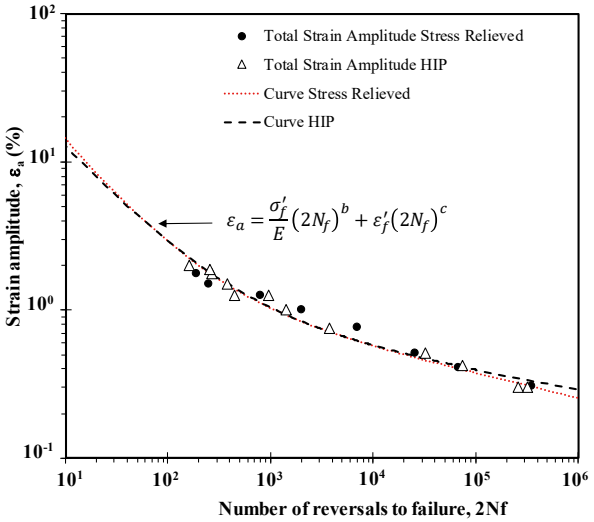

Fig. 6. Comparison of total strain amplitudes versus number of reversals to failure for both treatments.

4. Conclusions

- Stress relieved specimens exhibit significantly cyclic softening. However, for HIP specimens no significant change of the cyclic behavior in relation to the monotonic one was observed;
- Basquin and Coffin-Manson equations fits well the fatigue results under constant strain. The transition life was 187 reversals and 326 reversals, for stress relieved and HIP specimens, respectively;
- Significant differences were observed in cycle behavior for both treatments. Anyway, fatigue life for a given strain is governed mainly by the strain value, independently of the post manufacturing heat treatment.

Acknowledgements

The authors would like to acknowledge the sponsoring under the project no. 028789, financed by the European Regional Development Fund (FEDER), through the Portugal-2020 program (PT2020), under the Regional Operational Program of the Center (CENTRO-01-0145-FEDER-028789) and the Foundation for Science and Technology IP/MCTES through national funds (PIDDAC).

References

Edwards, P., Ramulu, M., 2014. Fatigue performance evaluation of selective laser melted Ti–6Al–4V. Mater Sci Eng A 598, 327–337.

Frazier, W.E., 2014. Metal additive manufacturing: a review, Journal of Materials Engineering and Performance 23, 1917–1928.

Greitemeier, D., Dalle, Donne C., Syassen, F., Eufinger, J., Melz, T., 2015. Effect of surface roughness on fatigue performance of additive manufactured Ti-6Al-4V. Mater Sci Technol 32:7, 629-634.

Greitemeier, D., Palm, F., Syassen, F., Melz, T., 2017. Fatigue performance of additive manufactured Ti-6Al-4V using electron and laser beam melting. International Journal of Fatigue 94, 211-217.

Guo, N., Leu, M.C., 2013. Additive manufacturing: technology, applications and research needs. Frontiers of Mechanical Engineering 8, 215–243.

Leuders, S., Thöne, M., Riemer, A., Niendorf, T., Tröster, T., Richard, H.A., et al., 2013. On the mechanical behaviour of titanium alloy TiAl6V4 manufactured by selective laser melting: fatigue resistance and crack growth performance. Int J Fatigue 48, 300–307.

Murr, L.E, Gaytan, S.M., Ceylan, A., Martinez, E., Martinez, J.L., Hernandez, D.H.., Machado, B.I., Ramirez, D.A., Medina, F., Collins, S., Wicker, R.B., 2010. Characterization of titanium aluminide alloy components fabricated by additive manufacturing using electron beam melting. Acta Materialia 58, 1887–1894.

Petrovic, V., Gonzalez, J.V.H., Ferrando, O.J., Gordillo, J.D., Puchades, J.R.B., Grinan, L.P., 2011. Additive layered manufacturing: sectors of industrial application shown through case studies. International Journal of Production Research 49, 1061–1079.

Rafi, H.K., Starr, T.L., Stucker, B.E., 2013. A comparison of the tensile, fatigue, and fracture behavior of Ti–6Al–4V and 15–5 PH stainless steel parts made by selective laser melting. Int J Adv Manuf Technol 69, 1299–1309.